

IMECE2012-87423

STRUCTURAL MICRO PROCESSING OF HAVERSIAN SYSTEMS OF A CORTICAL BOVINE  
FEMUR USING OPTICAL MICROSCOPE AND MATLAB

**Ilige S. Hage**

American University of Beirut  
Mechanical Engineering Department  
P.O. Box 11-0236, Riad El-Solh  
Beirut 1107 2020, Lebanon  
Email: ish07@aub.edu.lb

**Ramsey F. Hamade**

American University of Beirut  
Mechanical Engineering Department  
P.O. Box 11-0236, Riad El-Solh  
Beirut 1107 2020, Lebanon  
Email: rh13@aub.edu.lb

**ABSTRACT**

Processing of optical images of bone has been a topic of considerable interest in the past and continues to be so. Image processing can be used in medicine in order to improve the image visualization to detect diseases, and to compute properties such as area for abnormal cells. Several studies of bone images have been conducted using several methods including segmentation and image enhancement. The aim of this paper is to generate a standalone automated code for segmenting colored optical microscope images in order to show the microstructure of a cortical bone as a multi-phase (here 4 phases) composite: Lamella (matrix), Haversian canals, osteoblast lamella boundaries (freshly generated lamella lining), and lacunae (containing living cells).

For this purpose, we investigate the use of MATLAB, which contains image-processing toolboxes with many analytical capabilities that have been advertised to be useful for many applications including biological systems. In this work, such capabilities are utilized in image processing of the microstructure of bovine cortical bone, which is generally accepted as proxy for human bone. Two specimens of the cortical regions of a bovine femur bones were imaged using Olympus optical microscope. One of the specimens was treated with the Masson's trichrome staining treatment and the other with the Hematoxylin and Eosin (H&E) treatment. The images from the microscope were captured using a DP12 camera.

Furthermore, MATLAB results are contrasted against Stream®, a commercially available software package procured along with the Olympus optical microscope. Via color-coding to facilitate the bone microstructure identification, the image analysis results were compared

after computing the areas of each of the 4 constituent microstructural phases. Areas of each phase were calculated and comparisons made between the results obtained from the Stream® software and those obtained from MATLAB. The relative error was found to be quite small (<1%), which proves that MATLAB may be an effective software for medical image processing and may be the tool of choice for standalone applications.

**1. INTRODUCTION**

Bones are complex organic bio-composites characterized by multi-scale hierarchical structural geometry. Cortical bone is of special interest in this research. Figures 1 and 2 illustrate the salient features of such bones [1] as well as the micro details of the Osteon system [2].

**Compact Bone & Spongy (Cancellous Bone)**

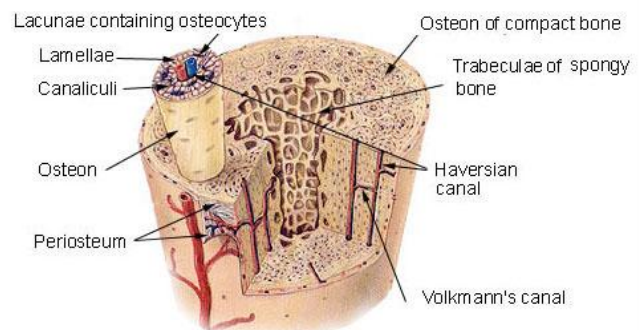


**Figure 1. Illustration of typical bone structure: highlighted are the compact and spongy regions [1].**

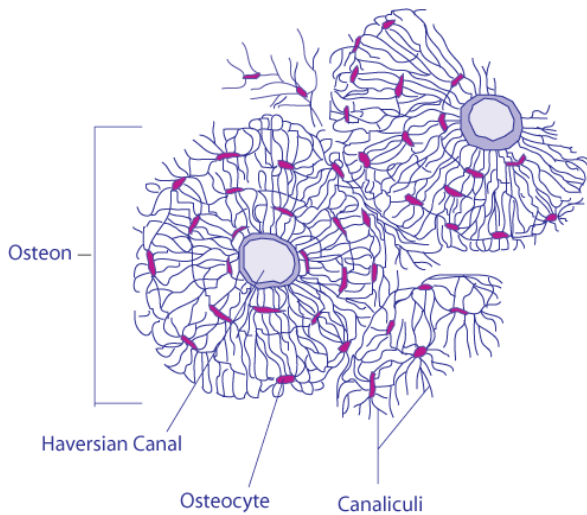


**Figure 2. Illustration of the details of the Osteon system [2].**

With the development of image processing of histological sections and in order to maximize the quality of the resulting images, many different sample preparation (staining) techniques have been utilized in the field. Two of the more commonly used being Masson's trichrome treatment and the Hematoxylin and Eosin (H&E) treatment. Automated bone image segmentation proved to be efficient in detecting microscopic bone features (e.g. osteons and Haversian canals) [3]. An example of a knowledge-based biomedical image analysis and comprehension system has been reported [4] which consider four major component blocks: (1) the entry-level pre-processing, (2) the low-level segmentation block, (3) the intermediate-level feature, and (4) the high-level interpretation block, proved its validity in improving medical imaging. A new hybrid automated gray scale segmentation technique combined with threshold and edge detection technique for effective and consistent extraction of bone features was developed [5]. This technique distinguishes normal from abnormal cells based on their shape definition. This segmentation and analysis technique was further applied to detect cancerous bone [6].

Although such studies have processed histological images in gray scale, the aim of this paper is to provide an automated processing technique of RGB color images (without the need to convert to gray scale). This technique is demonstrated below to be able of distinguishing the salient microstructural features of a bovine (cow) cortical bone, and of computing their respective areas. As such, this technique holds a major advantage over gray scale-based segmentation methods (e.g., [5,6]).

One advantage of this approach is our ability to present each of the segregated microstructural phases on a separate image as compared with techniques by other workers where all features were kept on one image.

Another advantage demonstrated in this study is that RGB is a natural technique typically used in light-emitting devices and that microscopy is a predominant analytical technique in medicine with colored digital cameras being a standard.

Another well recognized advantage of RGB-based processing over gray-scale-based processing is the fact that [7] RGB images provide more information through the color coding and the intensity because in RGB color space, chromaticities are represented by two values  $r$  and  $g$  which are related to  $R$ ,  $G$ , and  $B$  where  $R$ ,  $G$ , and  $B$  are defined as the intensity level of red, green, blue in RGB color space. This provides added sensitivity since these values are independent such that a small chromaticity change provokes a corresponding change in the values of  $r$  or  $g$  or in both. The normalized RGB performance is quite good because in the presence of a shadow the alteration of the ratio between the intensity values of basic colors  $R$ ,  $G$ ,  $B$  is negligible

## 2. MATERIALS AND SAMPLE PREPARATION

Material used in this study is cortical of a femur bone for a bovine animal (cow). Fresh bone sample was immersed in formaline solution during a 3-day period for softening and fixation. As a hole bone softening proved to be time consuming. The bone was cut into smaller pieces with electrical saw. Bone pieces were immersed in decalcifying solution surgipath (hydrochloric acid <15 %wt., EDTA (ethylenediaminetetraacetic acid disodium salt) < 5 %wt.) for 20 days. From the decalcified bone a cortex of 2mm thick were processed in a Leica machine model 300 where they were dehydrated and paraffin protected, after one day they were cut using a rotary microtome (model 340 E microm) finally they were rehydrated using hot water. For the purpose of better visualization two staining solutions for image optical enhancement were used 1- Masson's trichrome 2- Hematoxylin and Eosin (H&E).

## 3. IMAGE ACQUISITION AND BIOLOGICAL ASPECTS OF BONE

Olympus optical microscope was used with 20X magnification appropriate for bone microstructure recognition (resolution 50  $\mu\text{m}$ ). Micro images were acquired through DP12 camera with a resolution of 5 megapixels. Figure 3 shows samples of the acquired images: Figure 3 (top) Masson's trichrome and Figure 3 (bottom): Hematoxylin and Eosin (H&E) treatment. Both tested staining solutions provide a good enhancement for bone microstructure identifications perhaps with a slight edge for H&E. Lamella matrix, Haversian canals, osteoblast lamella boundaries (freshly generated lamella lining), and lacunae (containing living cells) are indicated by arrows in both figures: top for Masson's trichrome treatment and bottom for Hematoxylin and Eosin (H&E) treatment. Osteons are concentric cylinders surrounding the Haversian canals where blood runs, and

these canals along with the lamellae (with distributed lacunae) constitute the osteon system. Each phase has its chemical composition or mineralization that explains why the color intensity level differs; the regions that are less mineralized are darker [8].

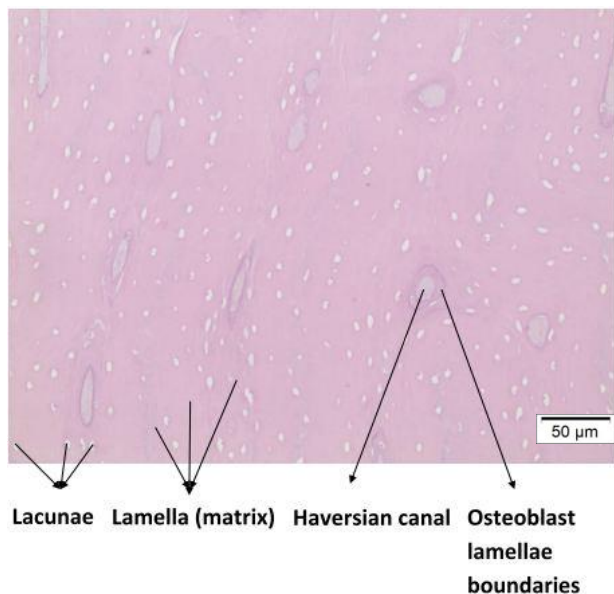
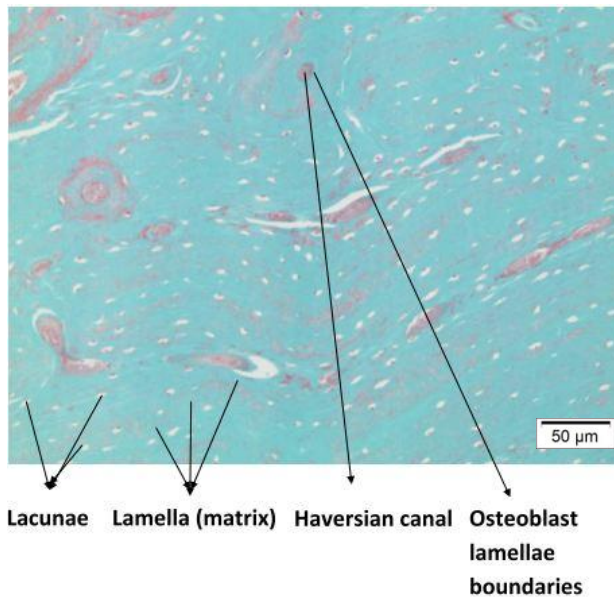


**Figure 3. Microstructures revealed: Masson's trichrome treatment (top); Hematoxylin and Eosin (H&E) treatment (bottom)**

#### 4. IMAGE PROCESSING AND ANALYSES

##### 4.1 RGB image acquisition and processing

RGB images were color thresholded based on intensity using the Stream® software package acquired along with the optical microscope (Soft imaging solution). Figures 4 and 5 show the color threshold

images for the Masson's trichrome staining and the H&E staining treatments, respectively.

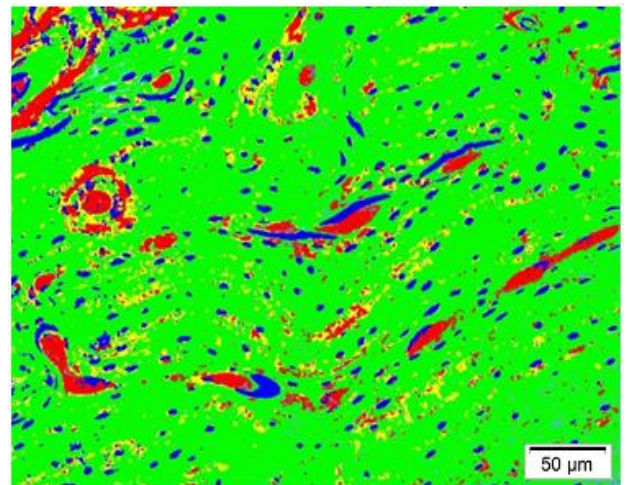


**Figure 4. Color threshold image from Stream® software for the Masson's trichrome staining**

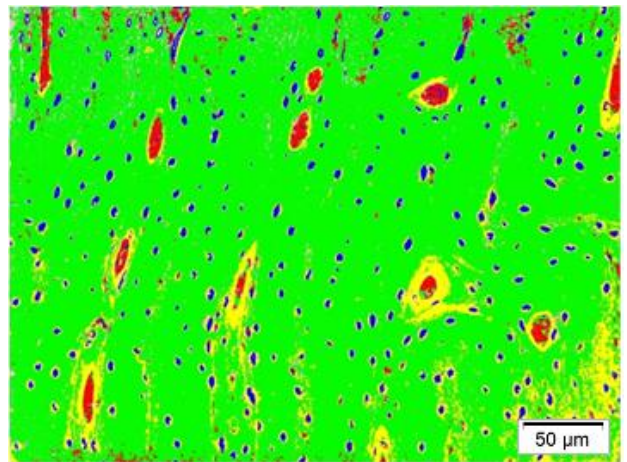


**Figure 5. Color threshold image from Stream® software for the H&E staining**

Since the quality of images are normally altered by several factors such as noise, defective pixels, and bad illumination, a procedure (originally outlined in Matlab tutorials) by which combining different MATLAB tools was recommended where image processing is divided into 2 parts: pre-processing and post-processing. For pre-processing, this is followed:

- 1- Contrast enhancement: to clearly identify different component of the microscopic image.
- 2- Correct bad illumination: in order to clearly identify the different patterns within the image.

Post-processing or morphological image processing procedure includes: segmentation based on K-means clustering for dividing the image in 4 regions focusing on each feature alone, and "regionprops" that can find properties for each region such as area in each cluster (illustrated in Figure 6).

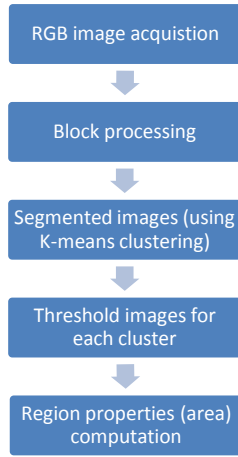


Figure 6. Methodology for microstructure analysis

#### 4.2 Block processing

For analyzing large images, block processing was used in order to speed up the image analysis procedure. Block processing toolbox divides the input image into blocks of the specified size, processes them by using the function handle one block at a time, and then assembles the results into an output image.

#### 4.3 Color-Based segmentation using K-Means clustering (pixel clustering)

The aim of this technique is to separate colors in an automated method by using the  $L^*a^*b^*$  color space and K-means clustering [9]. RGB images were imported into MATLAB and converted into 3d dimensional matrices. Converted images were clustered using the K-means clustering toolbox of MATLAB by following several steps, according to [10]. First, in order to enhance the analysis of the images, RGB images were converted into  $L^*a^*b^*$  Color Space images, where ‘L’ designates the luminosity, ‘a’ and ‘b’ designate the chromaticity layers, the coloring information is included in these layers. The ‘a’ and ‘b’ channels were separated. Then, partition clustering begins where division of data in similar groups and treatment of each object as having a location in space, begins. The partition is based on the sum of the squared Euclidian distances between the center of a cluster and the samples in the cluster

$$Q = \sum_{j=1}^k \sum_{i=1}^n \|v_i^j - \mu_j\|^2 \quad (1)$$

Where  $v_i^j$  is the  $i$ th sample of the  $j$ th class  $K_j$  and  $\mu_j$  the center of the  $j$ th cluster defined as the mean of  $v_i \in K_j$ [9]. Afterwards, the number of clusters  $K$  was previously specified as 4, (for each phase of the composite bone in order to separate it in 4 clusters partitioned), and the centroids  $\mu_j$  were initialized. Following, each pixel was assigned to a group with the nearest centroid. The centroids were then recalculated. These steps were repeated until the changing of centroids is eliminated.

#### 4.4 Thresholding

Images were thresholded by choosing the appropriate threshold value, is mandatory for isolating objects from their backgrounds in order to find the properties of these regions. According to [11], the optimal threshold is found using Otsu’s method or “graythresh” in MATLAB where the probability of distribution

$$p_i = \frac{n_i}{N} \quad (2)$$

where  $n_i$  the number of pixels with gray level  $I$ ,  $N$  is the total number of pixels,  $p_i$  is the probability of a pixel having gray level  $i$ .

$$\omega(k) = \sum_{i=0}^k p_i \quad (3)$$

$$\mu(k) = \sum_{i=k+1}^{L-1} p_i \quad (4)$$

where  $k$  is the threshold level,  $L$  is the number of gray scales.

$$\omega(k) + \mu(k) = \sum_{i=0}^{L-1} p_i = 1 \quad (5)$$

$K$  is found in a way to maximize the difference between  $\omega(k)$  and  $\mu(k)$ , this is done by finding the image average as

$$\mu_T = \sum_{i=0}^{L-1} i p_i \quad (6)$$

and finding  $k$  that maximizes the expression [11]

$$\frac{(\mu_T \omega(k) - \mu(k))^2}{\omega(k) \mu(k)}$$

#### 4.5 Area computations

Finally, for each image, areas were computed by using the “region props” function of MATLAB. Areas were converted from  $\text{pixel}^2$  into  $\mu\text{m}^2$ .

### 5. RESULTS

Figures 7 (Masson's trichrome staining treatment) and 8 (Hematoxylin & Eosin (H&E) treatment) represent the resulting images of the microstructures as segregated by Matlab. Shown in the figures are lacunae (in blue), Haversian canals (in red), lamellae (in green), the, and osteoblast lamella boundaries (in yellow). Areas were calculated for each color, and the sums of areas of each microstructural feature were calculated for each feature as well as aggregate areas.

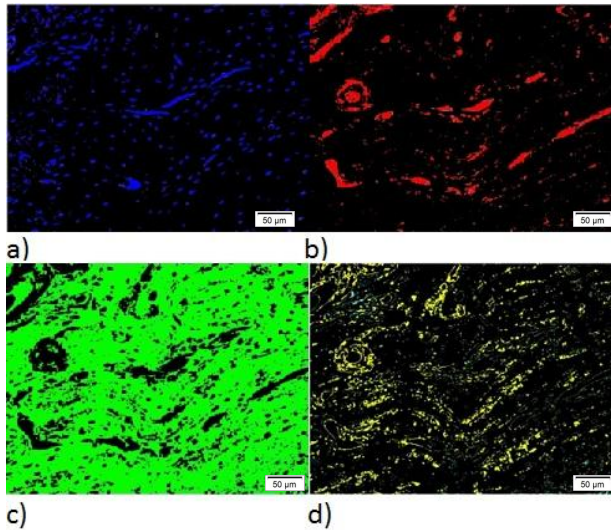


**Figure 7. Clusters obtained with MATLAB: a) objects in cluster 1 (lacunae), b) objects in cluster 2 (Haversian canals), c) objects in cluster 3 (Lamellae), d) objects in cluster 4 (osteoblast lamella boundaries):**

**Masson's trichrome treatment**

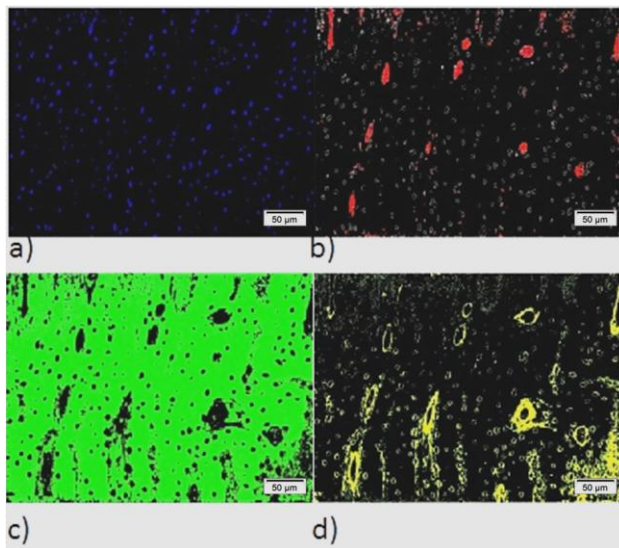


**Figure 8. Clusters obtained with MATLAB: a) objects in cluster 1 (lacunae), b) objects in cluster 2 (Haversian canals), c) objects in cluster 3 (Lamellae), d) objects in cluster 4 (osteoblast lamella boundaries):** H&E staining treatment.

## 5.1 Masson's trichrome staining treatment

**5.1.1 Results using Stream®** Figure 9 computes the sum of areas for each colored region (based on image in Figure 4).

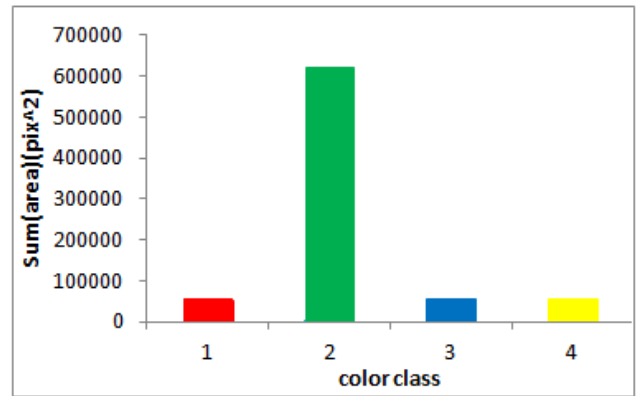


**Figure 9. Histogram of sum areas: Stream®**

Results are summarized in Table 1. Areas were calculated in  $(\mu\text{m})^2$  with respect to the scale bar that shows the resolution in  $\mu\text{m}$  and its dimension in pixels, and the dimension of the whole image in pixels.

**Table 1. Area and area fraction from Stream® software (OC (object class), A1 (Sum (Area) (pixel)<sup>2</sup>), A2 (Sum (Area) ( $\mu\text{m}$ )<sup>2</sup>), AF (Area fraction), ON (object count), ON% (object count percentage). R-H (red (Haversian canals)), G-L (green (lamellae)), B-L (blue (lacunae)), Y-O (yellow (osteoblast lamella boundaries)), S (Sum).**

Color	OC	A1(pixel <sup>2</sup> )	A2( $\mu\text{m}^2$ )	AF(%)	ON	ON (%)
R-H	1	52845	24791,24	6,69	1101	6,69
G-L	2	623966	292721,90	78,96	2100	78,96
B-L	3	56610	26557,52	7,16	694	7,16
Y-O	4	56836	26663,54	7,19	1620	7,19
S		790257	370734,19	100	5515	100

**5.1.2 Results using MATLAB** The 4 clusters obtained from Matlab were shown above in Figure 7 with histogram plot of aggregate areas is shown in Figure 10. In the figure, the x-axis represents the area in pixel<sup>2</sup> and y-axis (log scale) represents the number of objects.

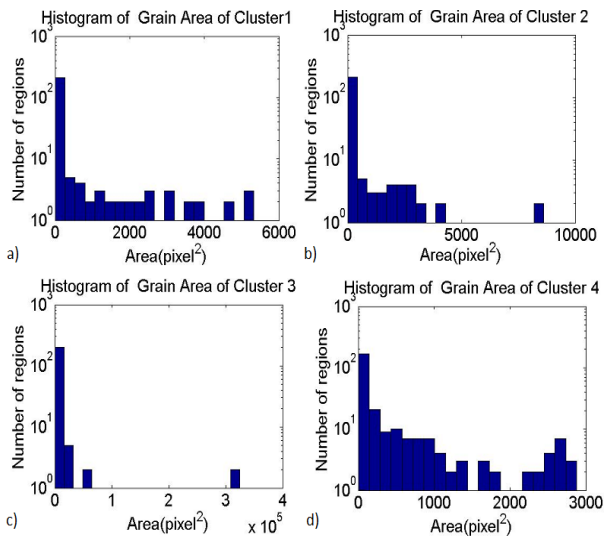


Figure 10. Histograms of grain areas with MATLAB (Y-axis is logarithmic scale) a) area in cluster 1, b) area in cluster 2, c) area in cluster 3, d) area in cluster 4.

**5.1.3 Comparisons** The areas in Table 2 were summed for each cluster, and calculated in  $(\mu\text{m})^2$ , and they were compared to the areas obtained from the Stream® software by calculating the relative percentage error (RE).

Table 2. Area and area fraction from MATLAB (OC (object class), A1 (Sum (Area) (pixel)<sup>2</sup>), A2 (Sum (Area) ( $\mu\text{m}$ )<sup>2</sup>), RE (relative percentage error). R-H (red (Haversian canals)), G-L (green (lamellae)), B-L (blue (lacuna)), Y-O (yellow (osteoblast lamella boundaries)), S (Sum).

Color	OC	A1(pixel <sup>2</sup> )	A2( $\mu\text{m}^2$ )	RE(%)
R-H	1	51168	24004,50	0,032
G-L	2	602833	282807,75	0,034
B-L	3	51445	24134,45	0,091
Y-O	4	65321	30644,12	0,149
S		770767	361590,82	0,0247

## 5.2. H&E staining treatment

**5.2.1 Results using Stream®** Figure 11 computes the sum of areas for each colored region (based on image in Figure 5).

These results are summarized in Table 3. Areas were calculated in  $(\mu\text{m})^2$  with respect to the scale bar that shows the resolution in  $\mu\text{m}$  and its dimension in pixels, and the dimension of the whole image in pixels.

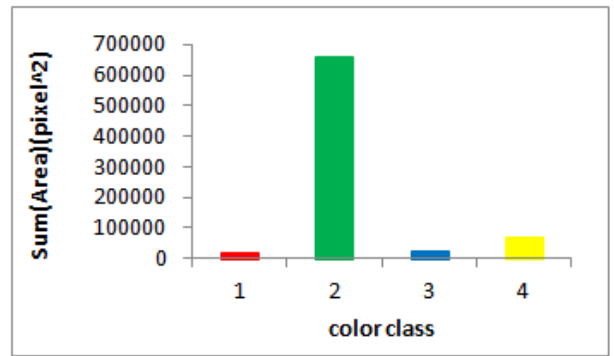


Figure 11. Histogram of sum areas- Stream®

Table 3. Area and area fraction from Stream® software (OC (object class), A1 (Sum (Area) (pixel)<sup>2</sup>), A2 (Sum (Area) ( $\mu\text{m}$ )<sup>2</sup>), AF (Area fraction), ON (object count), ON% (object count percentage). R-H (red (Haversian canals)), G-L (green (lamellae)), B-L (blue (lacuna)), Y-O (yellow (osteoblast lamella boundaries)), S (Sum).

Color	OC	A1(pixel <sup>2</sup> )	A2( $\mu\text{m}^2$ )	AF(%)	ON	ON (%)
R-H	1	20063	9412,2	2,57041	1796	35,13
G-L	2	663139	311099	84,96	1714	33,53
B-L	3	25425	11928	3,26	416	8,14
Y-O	4	71910	33735	9,21	1186	23,20
S		780537	366174	100	5112	100

**5.2.2 Results using MATLAB** The 4 clusters obtained from Matlab were shown above in Figure 8 with histogram plot of aggregate areas is shown in Figure 12. Where x-axis represents the area in pixel<sup>2</sup> and y-axis (log scale) represents the number of objects.

**5.2.3 Comparisons** The areas in Table 4 were summed for each cluster, and calculated in  $(\mu\text{m})^2$ , and they were compared to the areas obtained from the Stream® software by calculating the relative percentage error (RE).

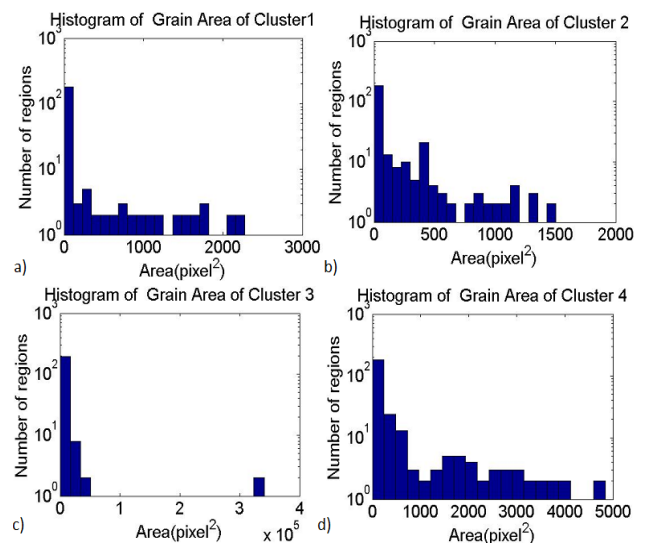


Figure 12. Histograms of grain areas with MATLAB. (Y-axis is logarithmic scale) a) area in cluster 1, b) area in cluster 2, c) area in cluster 3, d) area in cluster 4.

**Table 4. Area and area fraction from MATLAB (OC (object class), A1 (Sum (Area) (pixel)<sup>2</sup>), A2 (Sum (Area) (μm)<sup>2</sup>), RE (relative percentage error). R-H (red (Haversian canals)), G-L (green (lamellae)), B-L (blue (lacuna)), Y-O (yellow (osteoblast lamella boundaries)), S (Sum).**

Color	OC	A1(pixel <sup>2</sup> )	A2(μm <sup>2</sup> )	RE(%)
R-H	1	33925	15915,27	0,69
G-L	2	645115	302643,55	0,03
B-L	3	21783	10219,08	0,14
Y-O	4	83561	39201,07	0,16
S		784384	367978,98	0,005

## 7. SUMMARY AND CONCLUSIONS

In this MATLAB-based methodology for image process automation, bone images were analyzed through following steps:

- 1- The enhancement operations were applied to image.
- 2- The morphological operations were applied where a segmentation technique was used to enhance microscopic bone phase identification.
- 3- Threshold was applied
- 4- The average areas of phases were then calculated with respect to the total image area in terms of pixels and micrometers.

A demonstration of the effectiveness of MATLAB's image processing toolbox was presented. This system is able to segregate color bone image into 4 different desirable phases of the osteon system and to compute areas for each colored cluster. This was done without the need for converting the images into gray scale as done by others [6]. The results are almost identical when comparing processing via MATLAB and that of the Stream® software (procured along with the Olympus optical microscope) with the relative errors being less than 1%. This proves the effectiveness of MATLAB for analyzing and computing properties of medical images.

The image-processing algorithm using MATLAB developed can be a useful tool to speed up histological analyses especially when medical researchers are working on large numbers of digital images. Not only can MATLAB be used to compute the relative areas of micro biological features, but feature recognition may be further enhanced by including such distinguishing capabilities of MATLAB as shape recognition of microstructural features. This is the focus of work in progress by the authors.

## 8. ACKNOWLEDGMENTS

The authors would like to acknowledge the following AUB personnel: Mr. Charbel Seif (instructor in the Mechanical Engineering Department) and Dr. Ayman

Tawil M.D. (Anatomic and Clinical Pathology) for their useful help and guidance in this project.

## 9. REFERENCES

- [1] [http://upload.wikimedia.org/wikipedia/commons/3/34/Illu\\_compact\\_spongy\\_bone.jpg](http://upload.wikimedia.org/wikipedia/commons/3/34/Illu_compact_spongy_bone.jpg)
- [2] [http://upload.wikimedia.org/wikipedia/commons/7/75/Transverse\\_Section\\_Of\\_Bone.png](http://upload.wikimedia.org/wikipedia/commons/7/75/Transverse_Section_Of_Bone.png)
- [3] Liu, Z-Q., Liew, H. L. Clement, J. G., Thomas, C.D.L., 1999, "Bone Image Segmentation", IEEE Transactions on biomedical engineering, 46(5), pp. 565-573.
- [4] Dhawan, A.P., 1990, "A review on biomedical image processing and future trends", Computer Methods and Programs in Biomedicine, 31, pp. 141-183.
- [5] Jatti, A., 2010, "Segmentation of Microscopic Bone Images", International Journal of Electronics Engineering, 2(1), 2010, pp. 11-15.
- [6] Jatti, A., 2011, "Segmentation and analysis of osteosarcoma cancerous bone micro array images-1", International Journal of Information Technology and Knowledge Management, 4(1), pp. 195-200.
- [7] Nghiem A. T., Bremond F., Thonnat M., 2004, "Shadow removal in indoor scenes", Project Pulsar INRIA Sophia Antipolis France.
- [8] Liu, Z-Q., Austin, T., Thomas, C.D.L., Clement, J.G., 1996, "Bone feature analysis using image processing techniques", Computers in Biology and Medicine, 26(1), pp. 65-76.
- [9] Chitade, A.Z., Katiyar, S.K., 2010, "Colour based image segmentation using K-means clustering", International Journal of Engineering Science and Technology, 2(10), pp. 5319-5325.
- [10] Demirkaya, O., Asyali, M.H., Sahoo, P.K., 2009, "Image Processing with MATLAB: Applications in Medicine and Biology". Boca Raton: CRC Press.
- [11] McAndrew, A., 2004, "An introduction to digital image processing with MATLAB", Australia: Thomson Course Technology.